Supplement of

Groundwater storage dynamics and climate variability in the Lower Kutai Basin of Indonesia: reconciling GRACE ΔGWS to piezometry

Supplementary Figures and Tables

Table S1: Comparison of the three GRACE datasets: JPL, CSR, and GSFC.

GRACE data	JPL (RL06M)	CSR (RL06.3)	GSFC (RL06v2.0)
Effective resolution	3º	1º	1º
Spatial sampling	0.5º	0.25º	0.5º
Baseline period	2004-2009	2004-2009	2004-2010
Land and ocean separation	Coastline Resolution Improvement (CRI) filter.	There is no CRI filter applied as in the JPL version.	Similar to CSR, no CRI filter has been applied to the dataset.
Downscaling approach	A set of gain factors is provided separately to correct signal attenuation and restore the original terrestrial water storage (TWS) signals. These gain factors are derived from the CLM hydrology model, which operates at a 0.5° spatial resolution. A least-squares fitting method is employed to align the 'mascon-averaged' hydrology model with the original 3° resolution data.	The data were originally estimated in the 1° geodesic grid domain but were resampled and released as 0.25° grids.	The 1° data have been resampled onto 0.5° grids. Land values are computed using a least-squares estimator.
Direct use	Users need to apply the optional gain factors for the 0.5º grids.	Users do not need to apply postprocessing or scaling factors to the GRACE data, as these solutions can be used as-is for their applications.	No postprocessing or scaling factors are required. The data are ready to be used as-is.
Notes for using the data	Although the data are represented on 0.5° grids, neighboring grids are not entirely independent of each other. The provided gain factors are suitable for hydrology-related signals but should not be applied to mountain glaciers or ice sheets.	Although the mascon solutions appear to have a resolution of ~120 km, the effective resolution is constrained by the fundamental spatial limitation of GRACE, roughly equivalent to a 300 km radius Gaussian smoother. The dataset should only be used for basin-scale analyses and should not be applied to a single grid point. Users should exercise caution when using the dataset for basins smaller than ~200,000 km².	Unlike the JPL and CSR datasets, no explicit notes are provided regarding the use of this dataset. However, the fundamental resolution of ~300 km should constrain the applications of this data.
References	Watkins et al. (2015); Landerer and Swenson (2012); Wiese et al. (2016) Website: https://grace.jpl.nasa.gov/data/get-data/jpl_global_mascons/	Save et al. (2016) Website: https://www2.csr.utexas.edu/grace/RL0603_mascons.html	Loomis et al. (2019) Website: https://earth.gsfc.nasa.gov/geo/data/grace-mascons

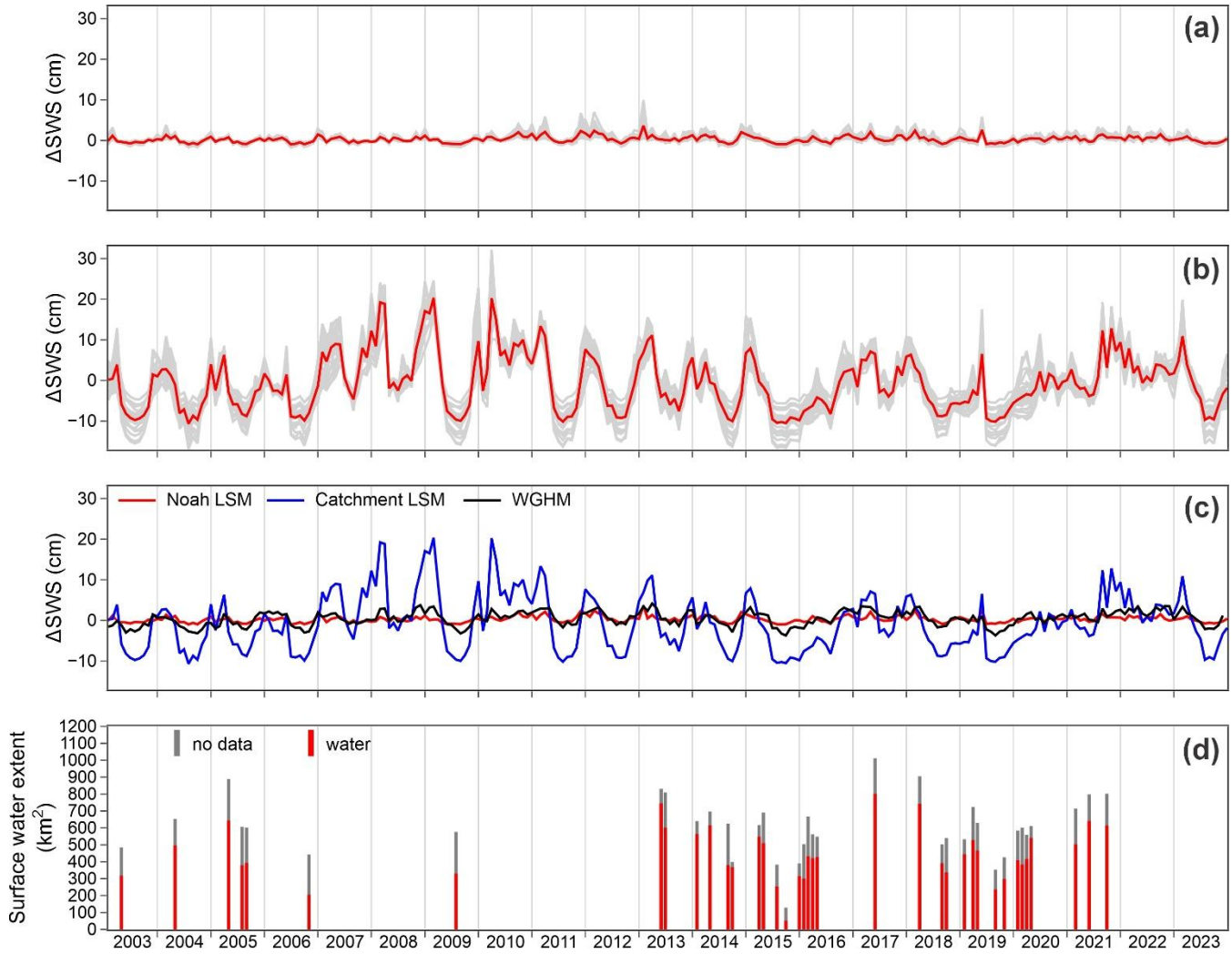

Figure S1: Comparison of ΔSWS between (a) Noah LSM, (b) Catchment LSM, and (c) the ensemble of both LSMs and the WGHM dataset. In panels (a) and (b), gray lines represent uncertainty derived from the composite ΔSWS of both LSMs, whereas red lines indicate the mean ΔSWS. In panel (c), the black line shows the mean ΔSWS from WGHM, and the red and blue lines correspond to the mean ΔSWS from Noah and Catchment LSMs, respectively. Panel (d) displays surface water extent (red bars) from Pekel et al. (2016), with gray bars indicating areas with ≤20% missing data.

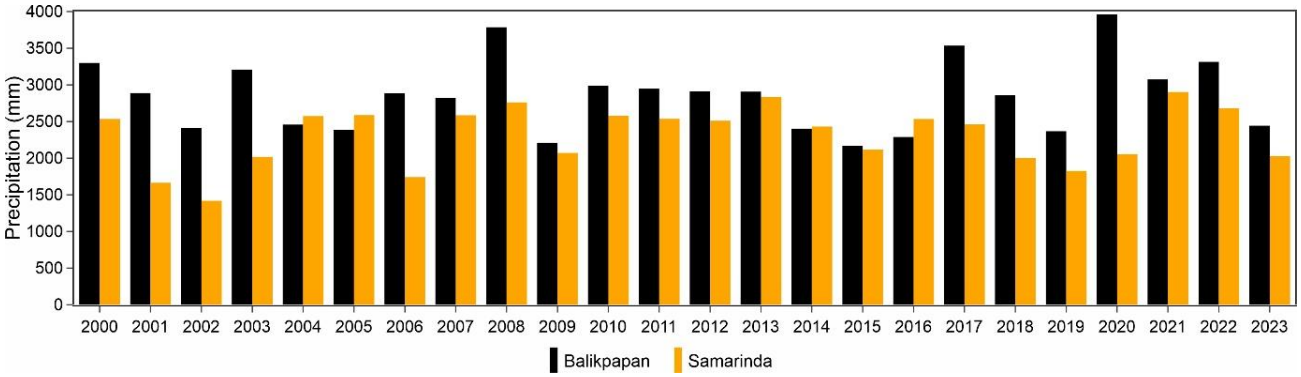

Figure S2: Annual precipitation recorded at Balikpapan and Samarinda stations.

10

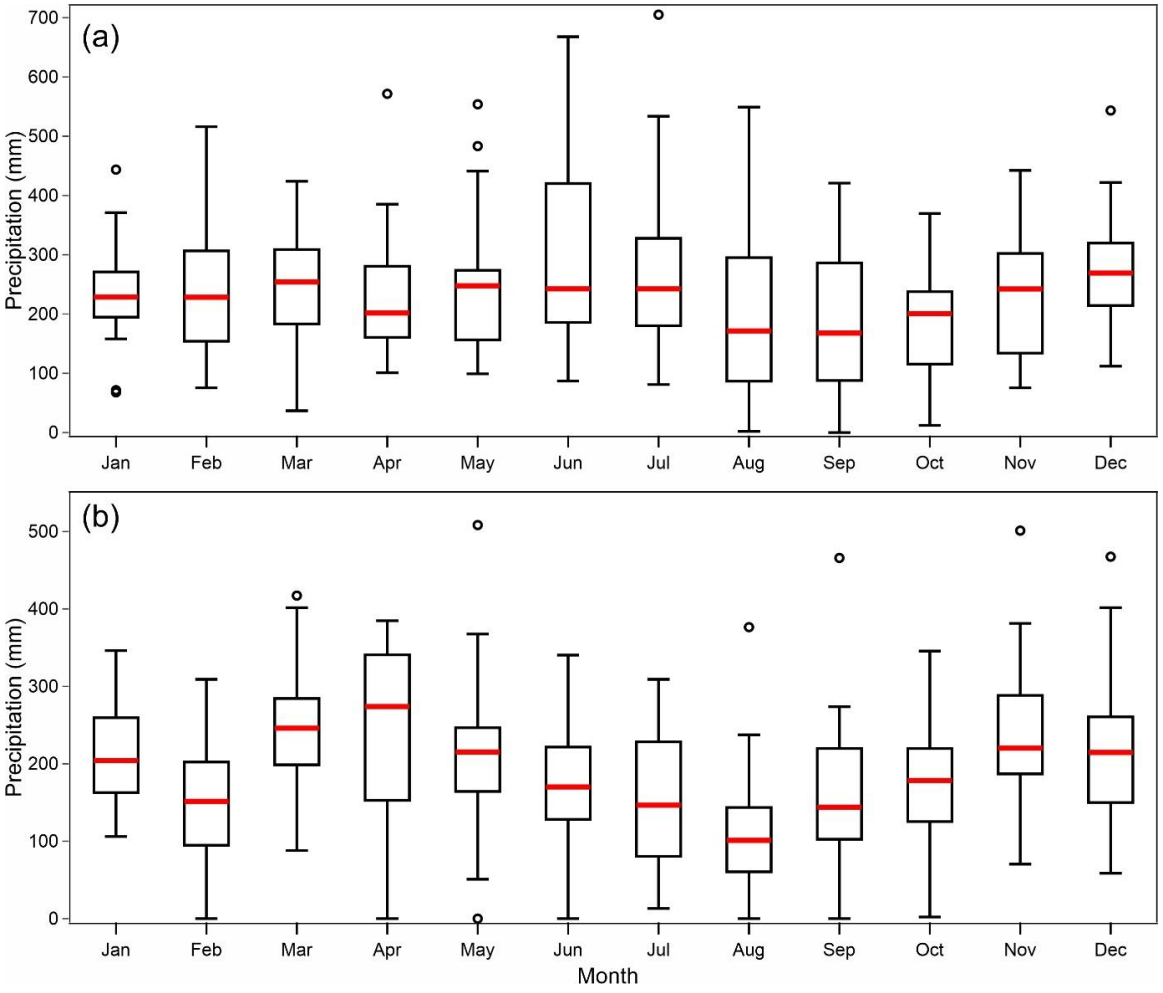

Figure S3: Boxplots of monthly precipitation at (a) Balikpapan and (b) Samarinda stations over a 24-year period (2000-2023). Red lines indicate median values.

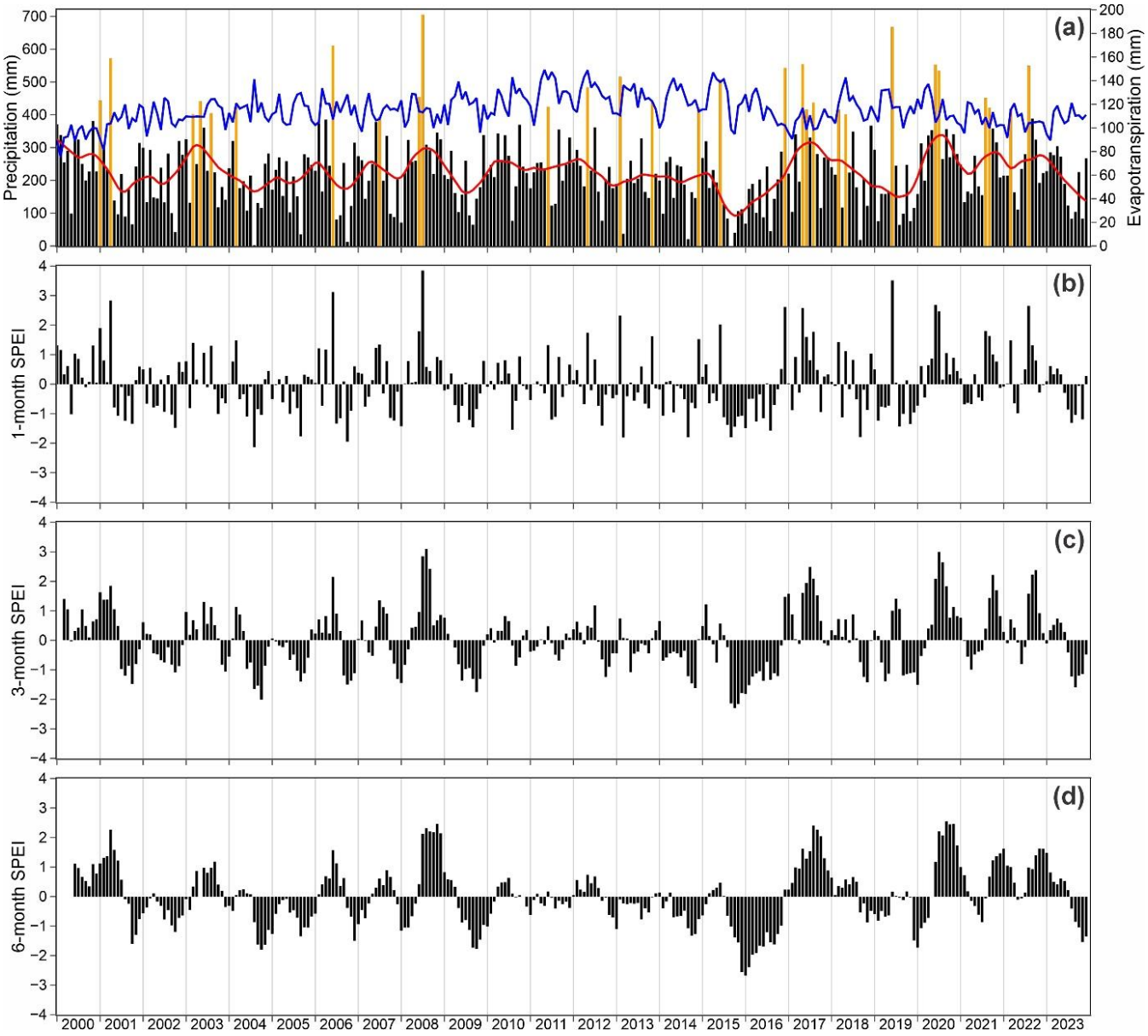

15 **Figure S4: (a) Monthly rainfall records (black and orange bars) at Balikpapan station. Orange bars indicate extreme rainfall events (>90th percentile), whereas the red line represents the precipitation trend derived using LOESS. Evapotranspiration from Noah LSM is shown as a blue line in (a). Plots (b) to (d) display the calculated SPEI.**

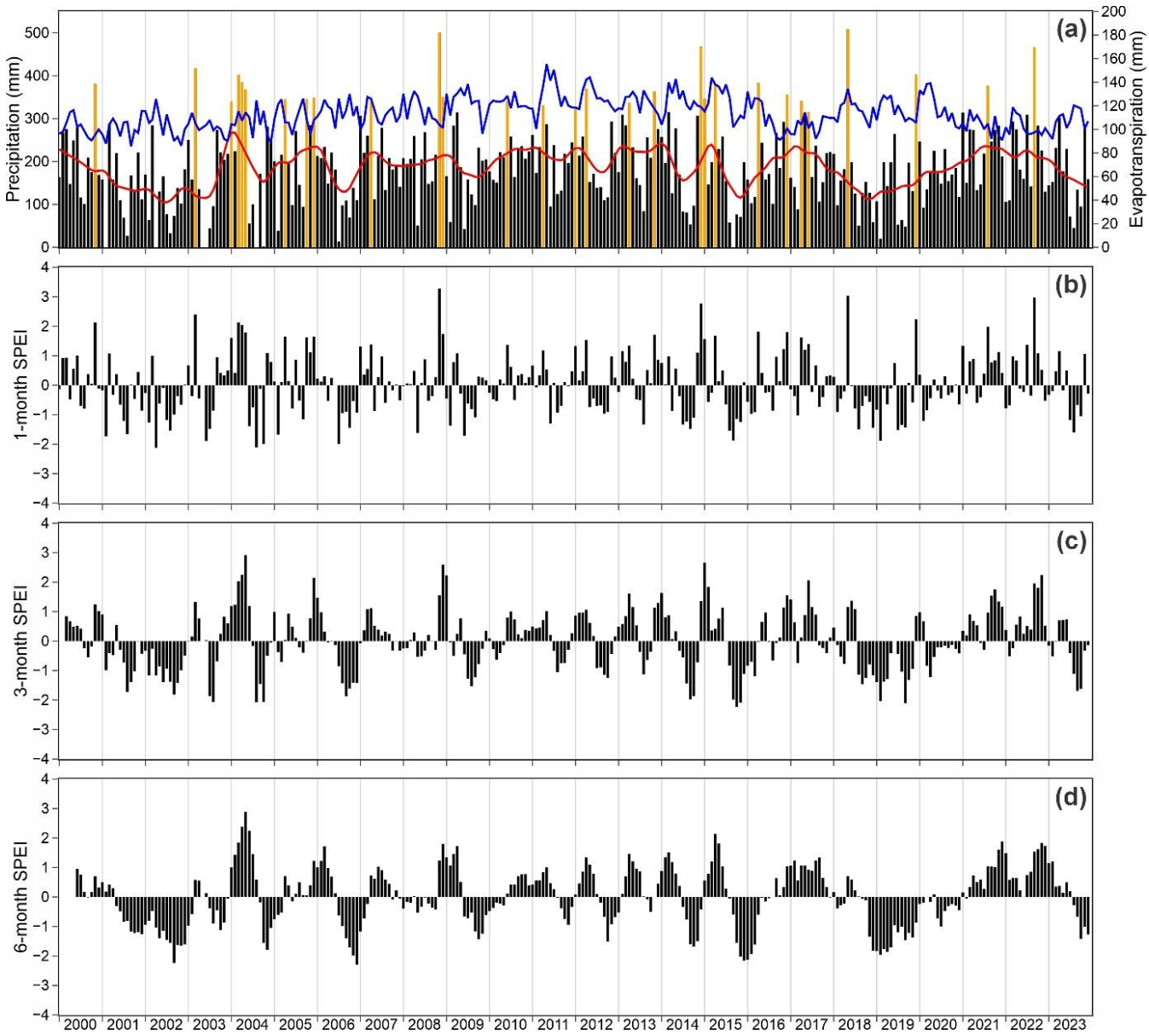

Figure S5: (a) Monthly rainfall records (black and orange bars) at Samarinda station. Orange bars indicate extreme rainfall events (>90th percentile), whereas the red line represents the precipitation trend derived using LOESS. Evapotranspiration from Noah LSM is shown as a blue line in (a). Plots (b) to (d) display the calculated SPEI.

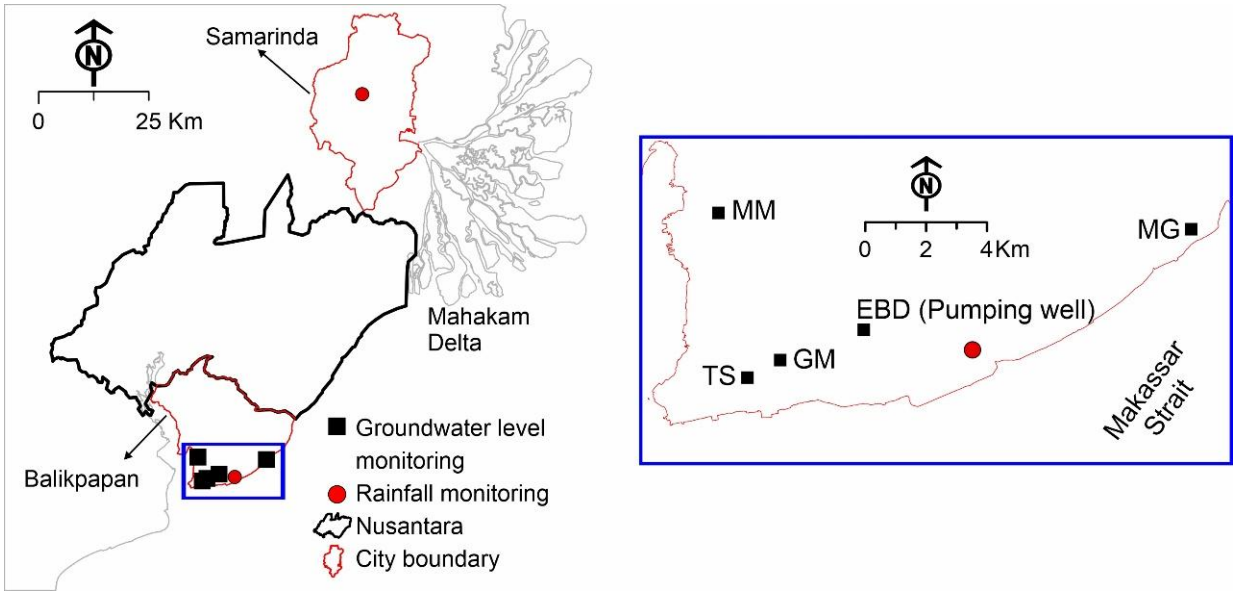

Figure S6: Map showing the locations of groundwater level monitoring sites.

25

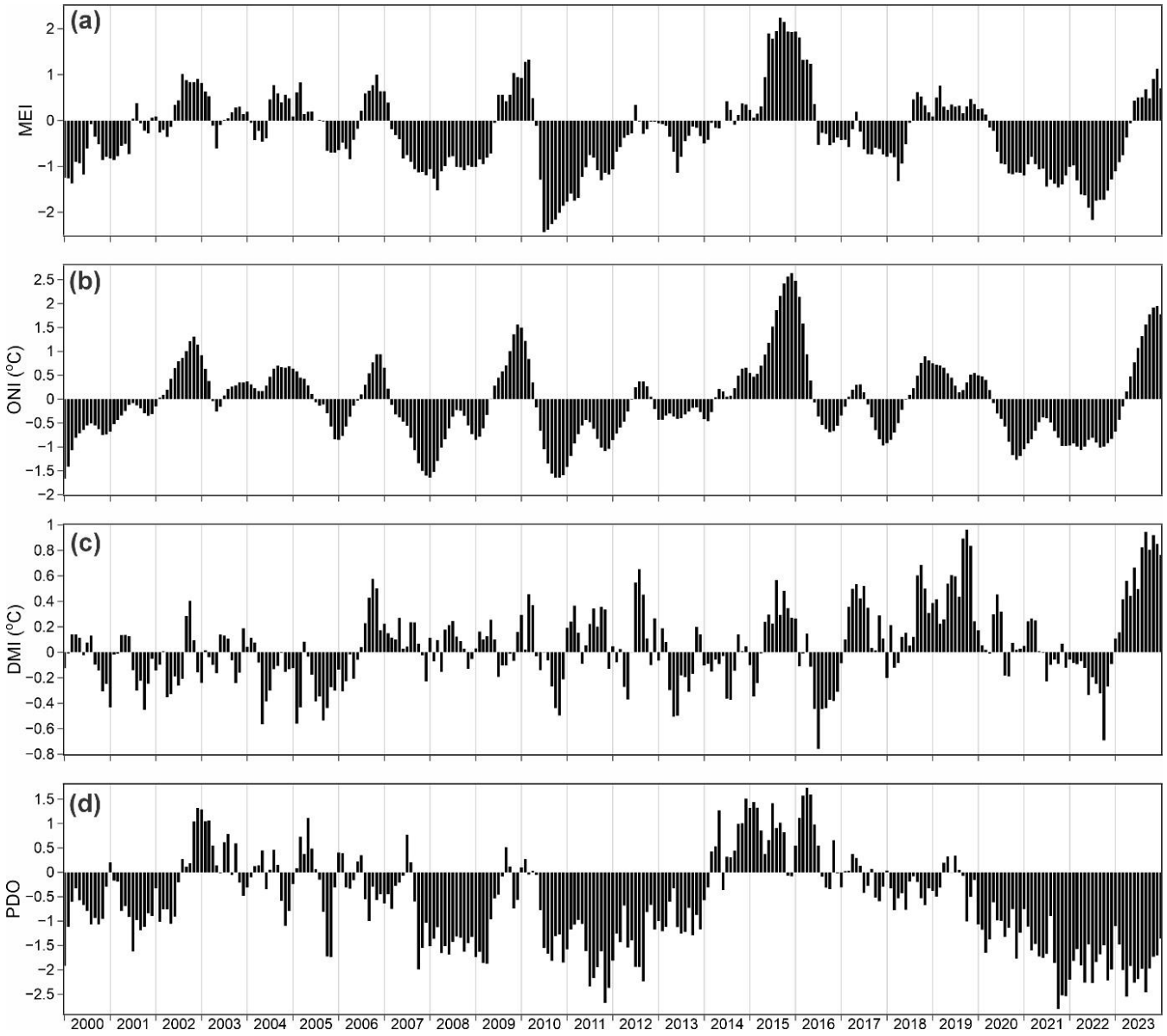

Figure S7: Four climate indices used in this study: (a) MEI, (b) ONI, (c) DMI, and (d) PDO. The indices were retrieved from the NOAA PSL portal (https://psl.noaa.gov/).

30

Table S2: Correlation coefficients (r) and root mean square error (RMSE) between GRACE datasets used in this study.

GRACE datasets	Grids	Correlation (r)	RMSE (cm)
JPL	Study area vs 1 Mascon	1.00	0.8
	Study area vs Borneo	0.96	1.8
GSFC	Study area vs 1 Mascon	0.96	2.5
	Study area vs Borneo	0.85	4.4
CSR	Study area vs 1 Mascon	0.98	1.2
	Study area vs Borneo	0.87	2.5

Table S3: Statistical comparison of GRACE datasets employed in this study.

GRACE datasets	Grids	mean	std	min	Q1	Q2	Q3	max	Skewness
JPL	Study area	3.2	5.6	-11.5	-0.4	3.7	7.0	17.2	-0.34
	1 Mascon	3.6	6.3	-12.9	-0.4	4.1	7.8	19.3	-0.34
	Borneo	3.1	4.5	-9.1	0.3	3.0	6.3	14.5	-0.07
GSFC	Study area	2.2	7.6	-23.7	-2.1	3.4	7.7	13.8	-1.03
	1 Mascon	3.0	6.1	-15.5	-0.8	3.9	7.3	15.5	-0.69
	Borneo	1.9	4.6	-12.1	-0.8	2.1	5.0	14.0	-0.31
CSR	Study area	1.5	5.1	-15.5	-0.9	2.8	4.8	13.3	-0.97
	1 Mascon	2.1	5.0	-14.9	-0.4	2.9	5.0	14.6	-0.64
	Borneo	2.0	4.5	-12.3	-0.9	2.6	4.9	13.8	-0.45

Table S4: Statistical comparison of GLDAS and WGHM datasets employed in this study.

GLDAS datasets	Parameters	mean	std	min	Q1	Q2	Q3	max	Skewness
Noah LSM	ΔSMS	-0.4	5.5	-28.8	-2.5	1.7	3.2	5.5	-1.93
	ΔCW	-0.003	0.007	-0.025	-0.007	-0.002	0.002	0.011	-0.64
	ΔSWS	0.3	0.8	-1.0	-0.3	0.2	0.7	3.7	0.80
Catchment LSM	ΔSMS	-0.5	4.1	-14.3	-3.2	1.3	2.6	4.1	-1.06
	ΔCW	-0.003	0.008	-0.022	-0.008	-0.002	0.002	0.018	0.04
WGHM	ΔSWS	0.4	1.8	-3.7	-0.9	0.6	1.7	4.1	-0.18

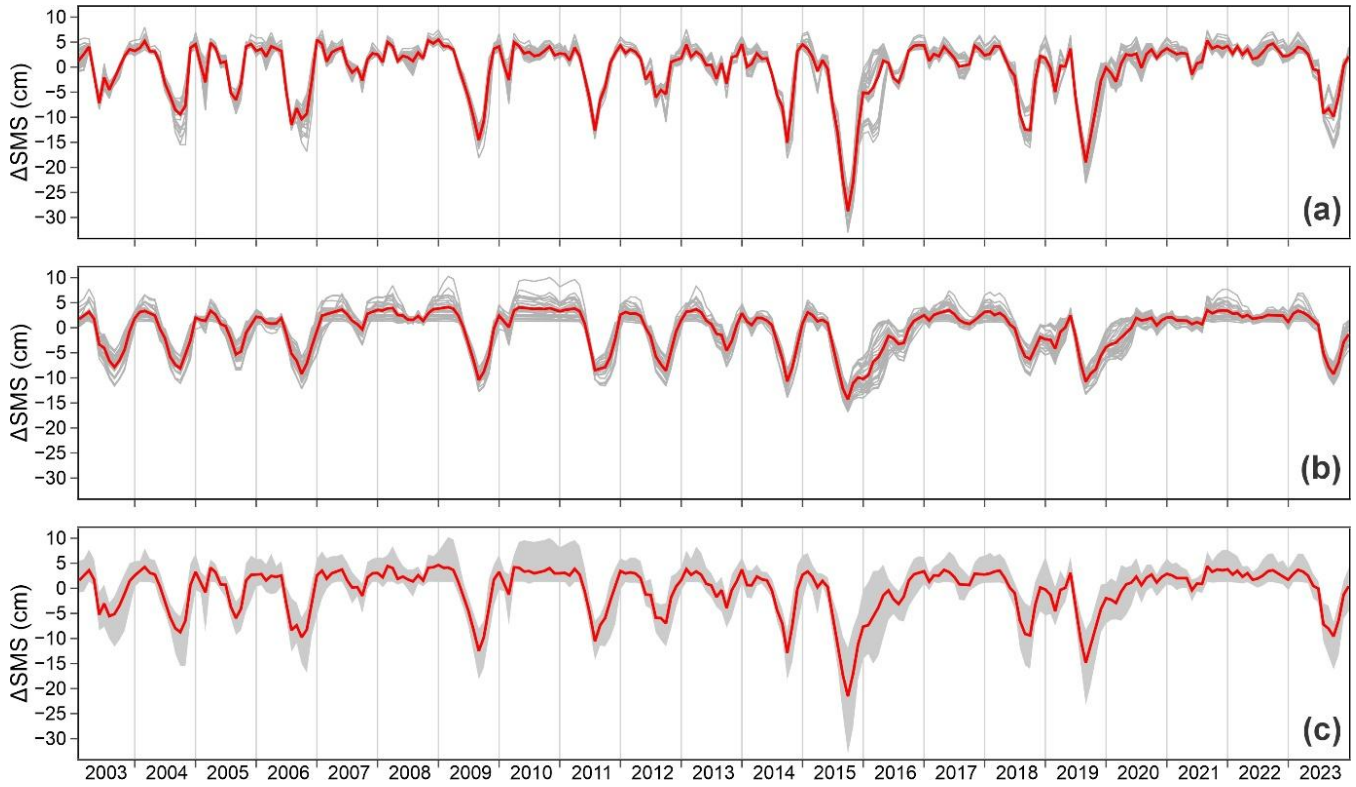

Figure S8: Comparison of ΔSMS between (a) Noah LSM, (b) Catchment LSM, and (c) the ensemble of both datasets. In (a) and (b), gray lines represent ΔSMS for each grid, whereas in (c), the gray shading indicates uncertainty derived from the composite ΔSMS of both GLDAS datasets. The red lines in (a) to (c) represent mean values.

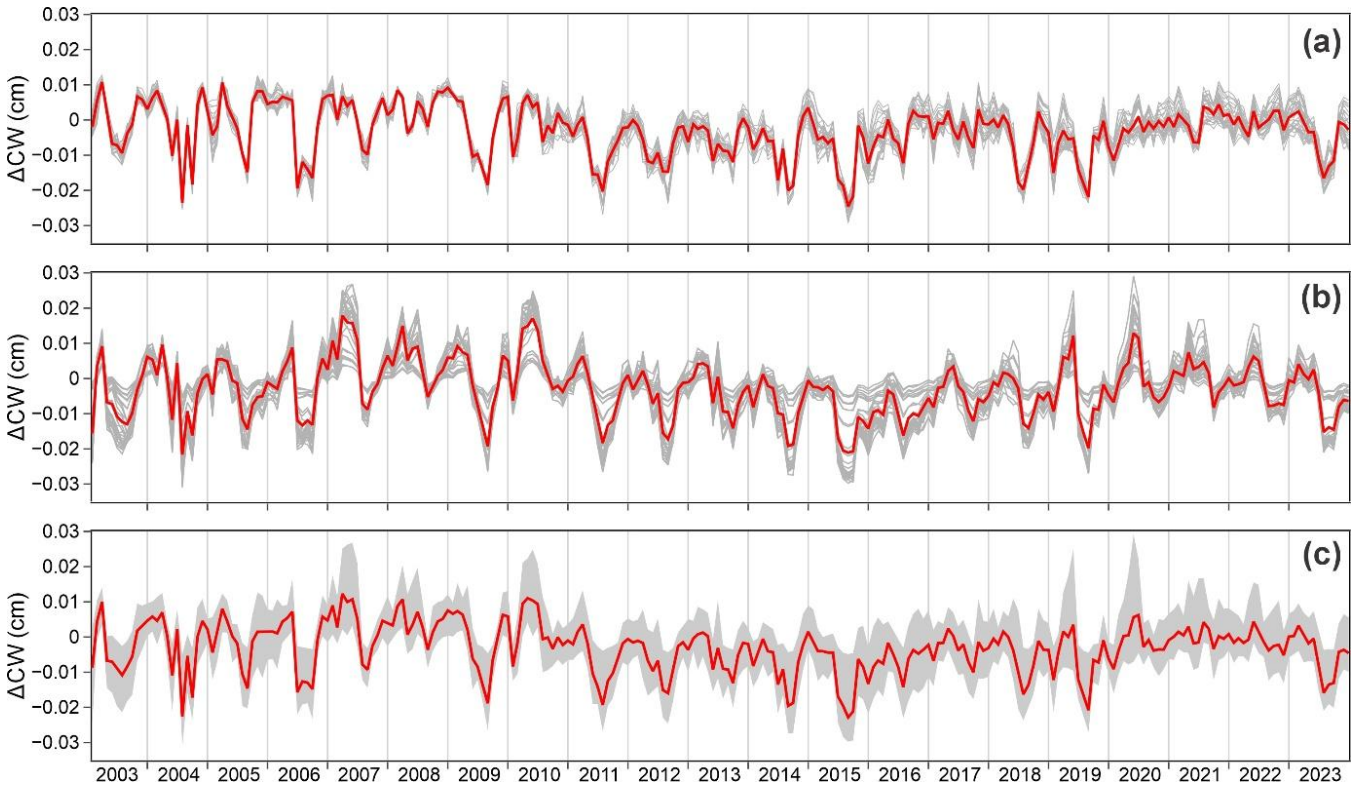

Figure S9: Comparison of ΔCW between (a) Noah LSM, (b) Catchment LSM, and (c) the ensemble of both datasets. In (a) and (b), gray lines represent ΔCW for each grid, whereas in (c), the gray shading indicates uncertainty derived from the composite ΔCW of both GLDAS datasets. The red lines in (a) to (c) represent mean values.

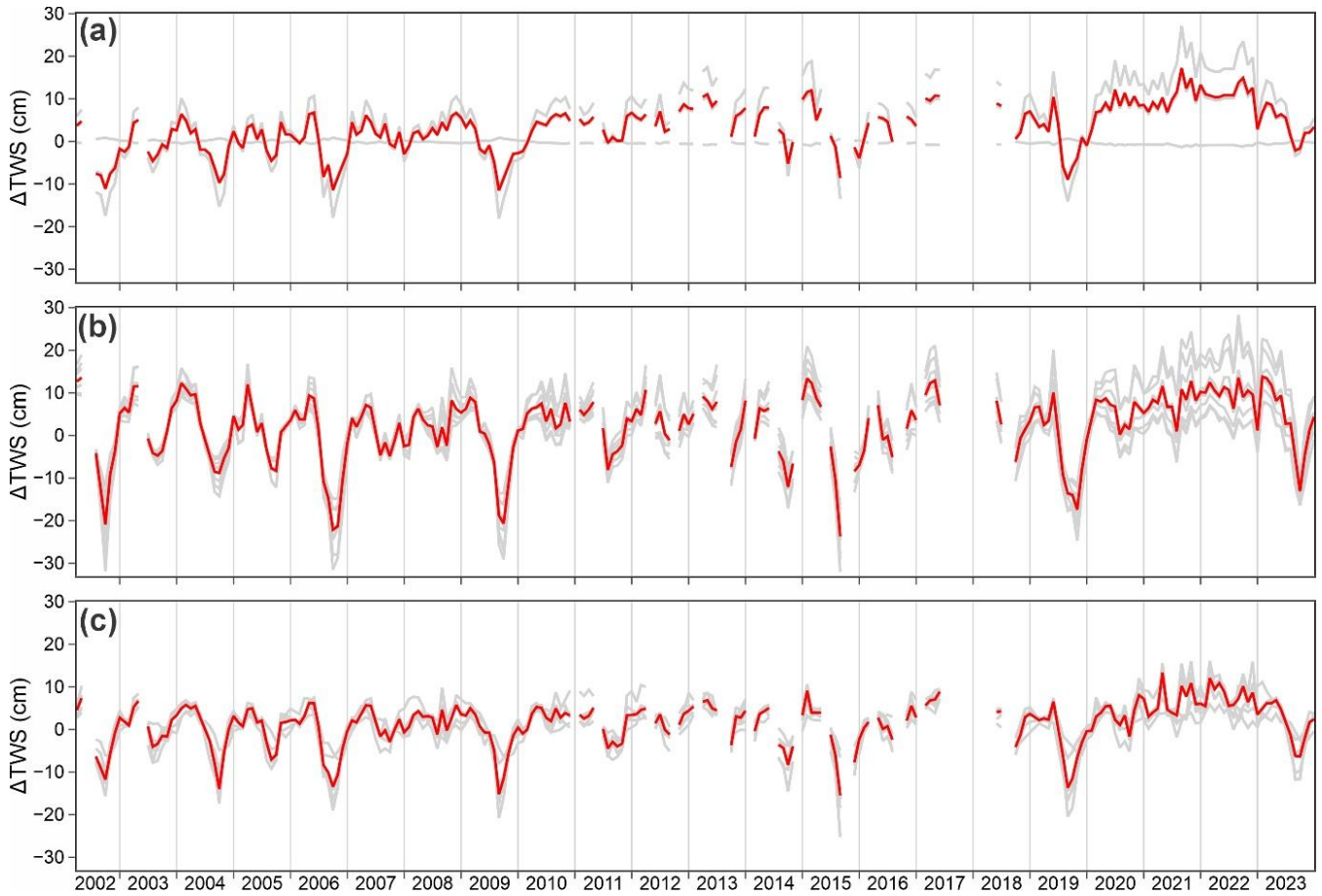

Figure S10: Comparison of ΔTWS between GRACE datasets: (a) JPL, (b) GSFC, and (c) CSR across eight 0.5° grids (JPL and GSFC) and the corresponding finer 0.25° grids (CSR). In (a) to (c), red lines represent mean values, whereas gray lines indicate ΔTWS for each grid.

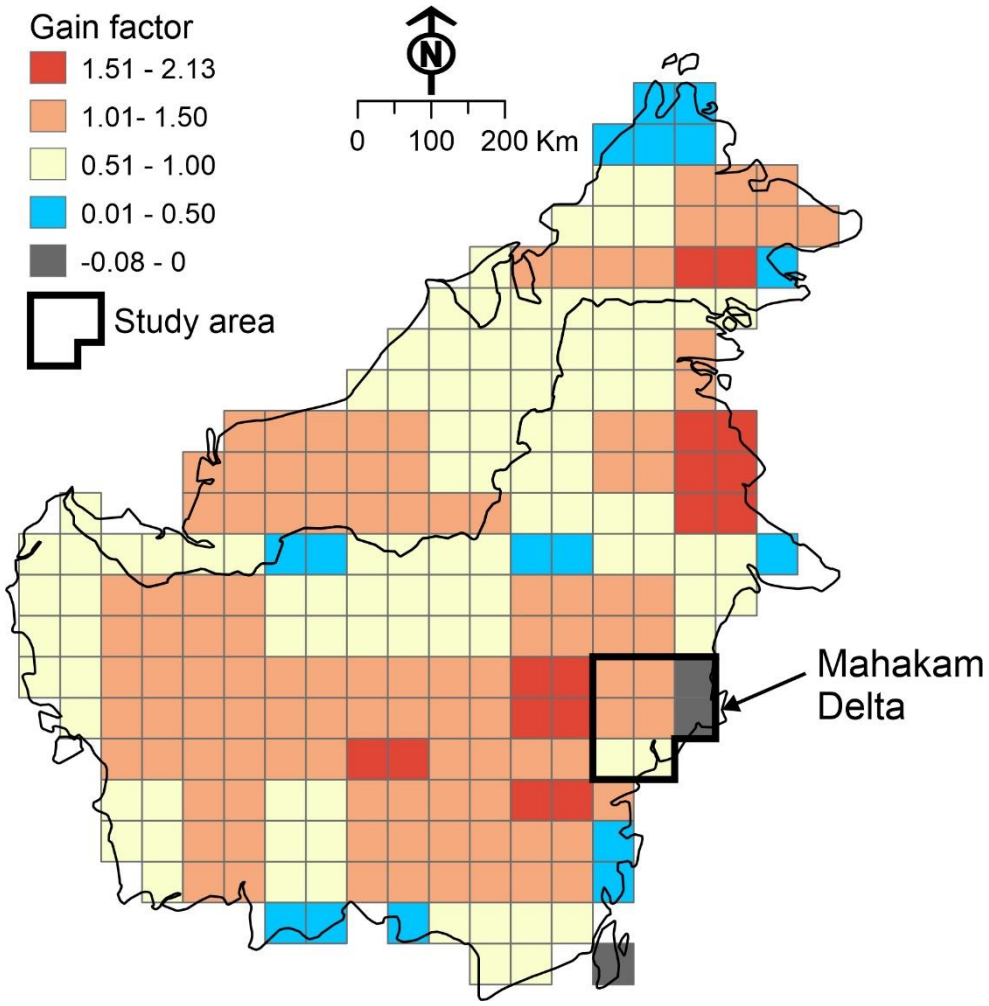

Figure S11: Distribution of gain factors in the GRACE JPL dataset. Negative gain factors are indicated in dark gray.

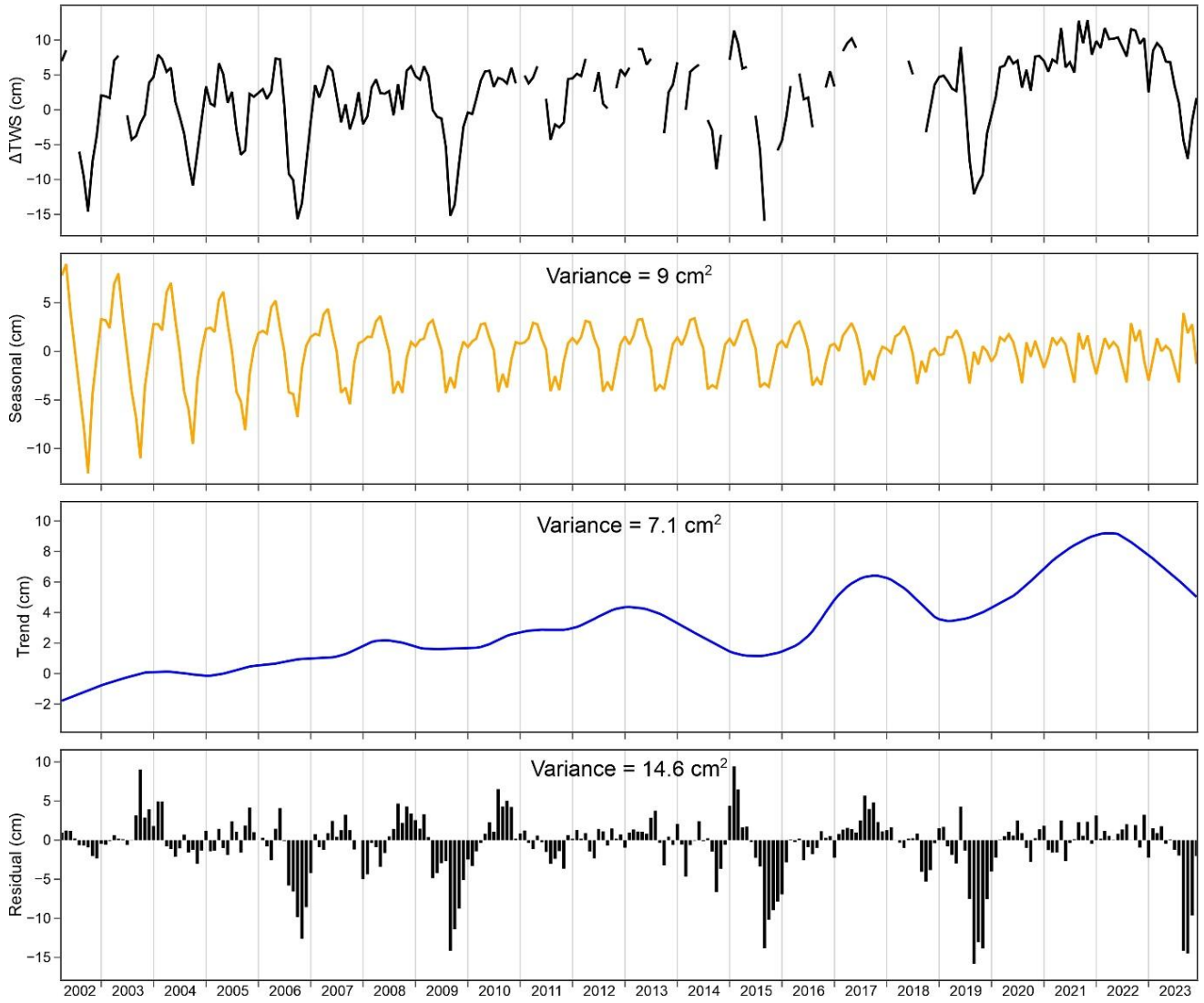

Figure S12: STL analysis results for the mean ensemble ΔTWS derived from the three GRACE datasets: JPL, GSFC, and CSR.

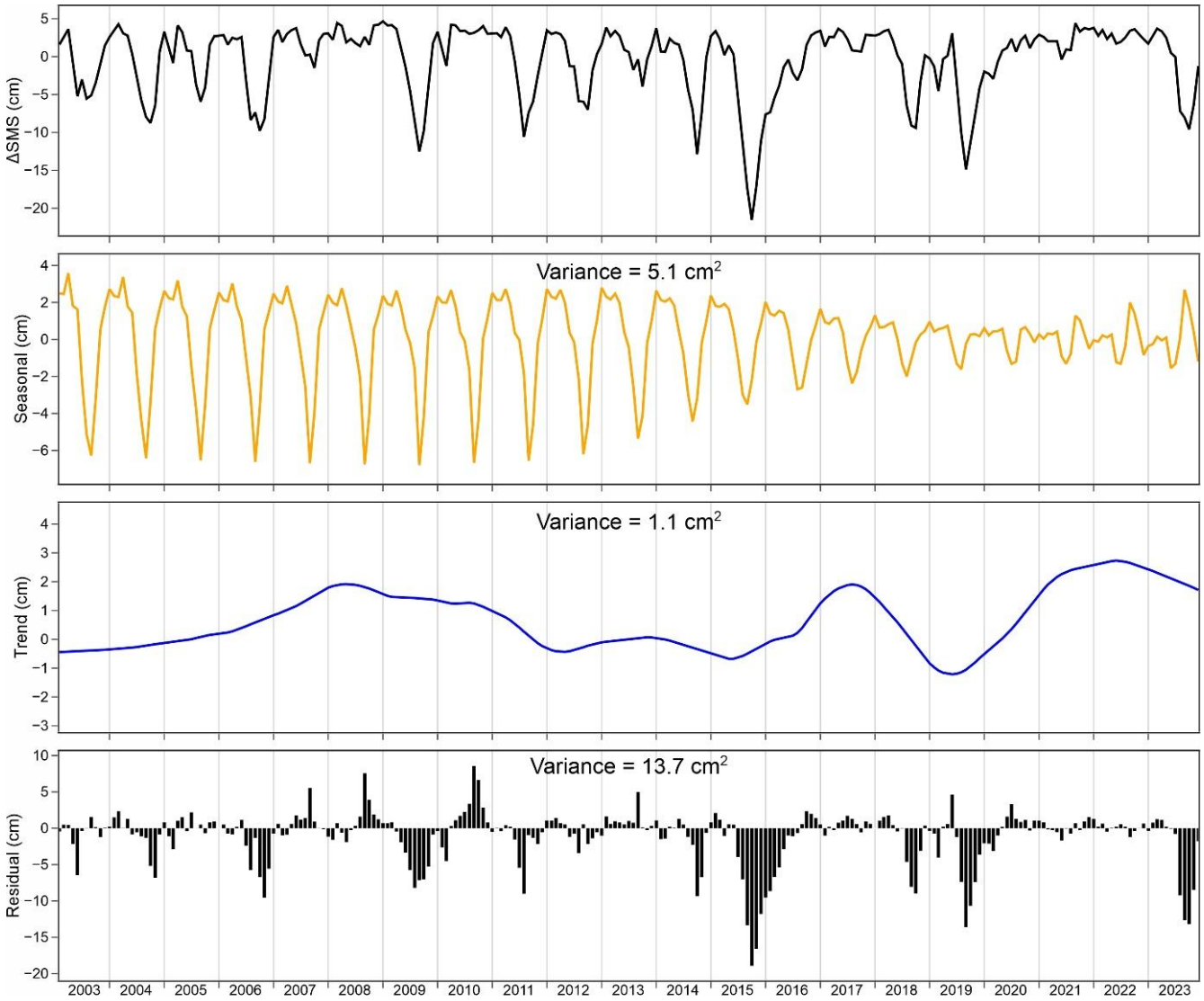

Figure S13: STL analysis results for the mean ensemble ΔSMS derived from the two GLDAS datasets: Noah and Catchment LSMs.

Table S5: Percentage of arithmetically implausible ΔGWS estimates for each of the 36 realizations, categorized by the specific implausibility criteria.

Realizations	Implausible ΔGWS (%)	Realizations	Implausible ΔGWS (%)	Realizations	Implausible ΔGWS (%)	Realizations	Implausible ΔGWS (%)
1	33	**11**	24	**21**	32	**31**	43
2	26	**12**	32	**22**	30	**32**	35
3	37	**13**	32	**23**	25	**33**	50
4	32	**14**	27	**24**	32	**34**	35
5	26	**15**	34	**25**	24	**35**	26
6	37	**16**	27	**26**	17	**36**	39
7	29	**17**	21	**27**	28		
8	20	**18**	31	**28**	39		
9	34	**19**	28	**29**	32		
10	30	**20**	23	**30**	45		

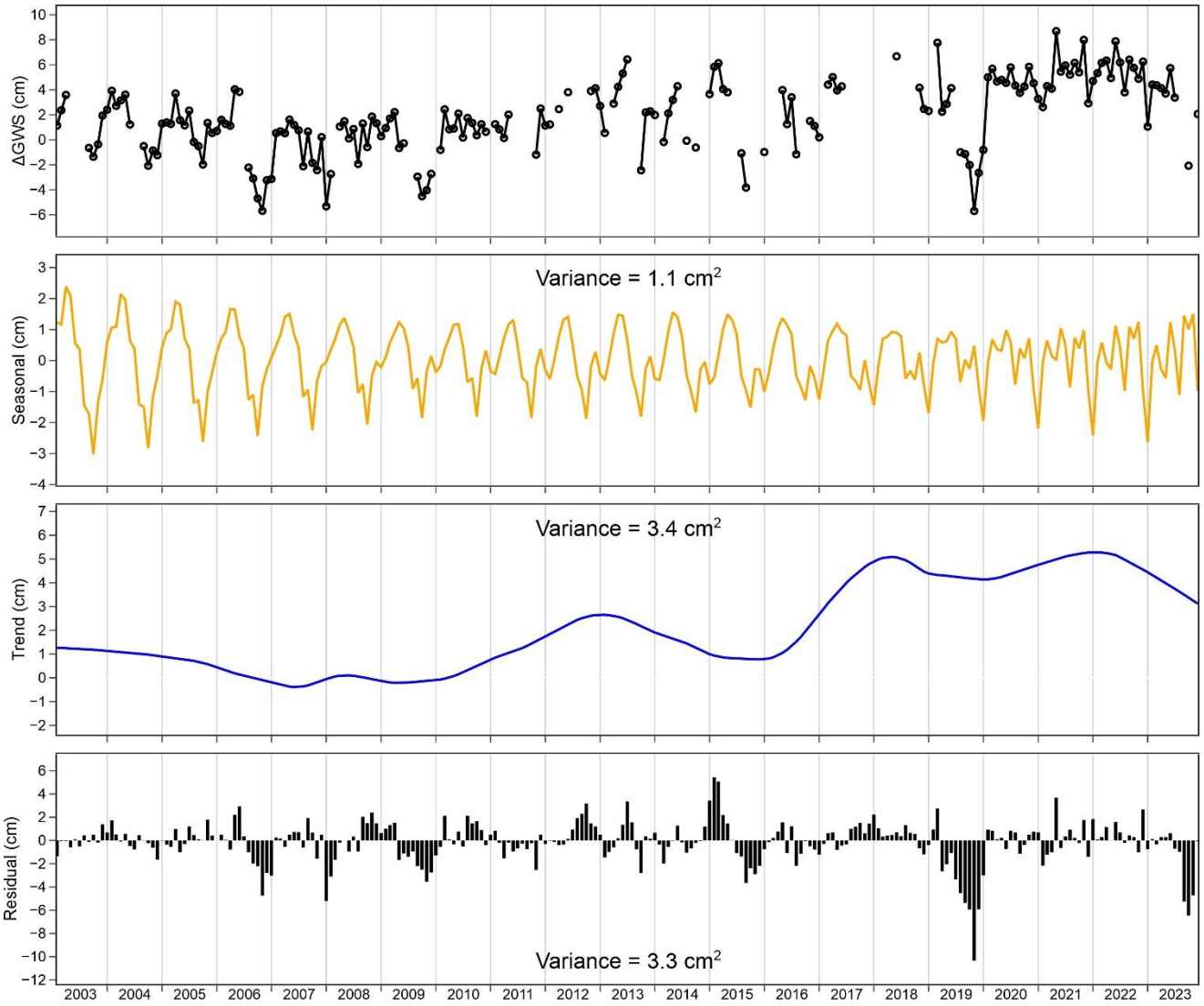

Figure S14: STL analysis results for mean ensemble ΔGWS computed from 36 realizations.

80

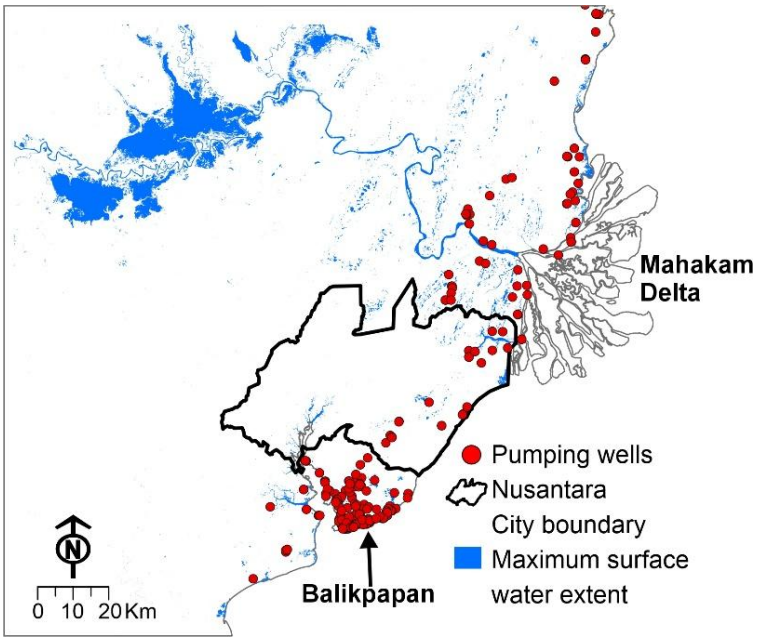

Figure S15: Distribution of registered pumping wells in the coastal part of the study area. The data are obtained from the Indonesian Geological Survey (2023). The surface water extent is from Pekel et al. (2016).

85

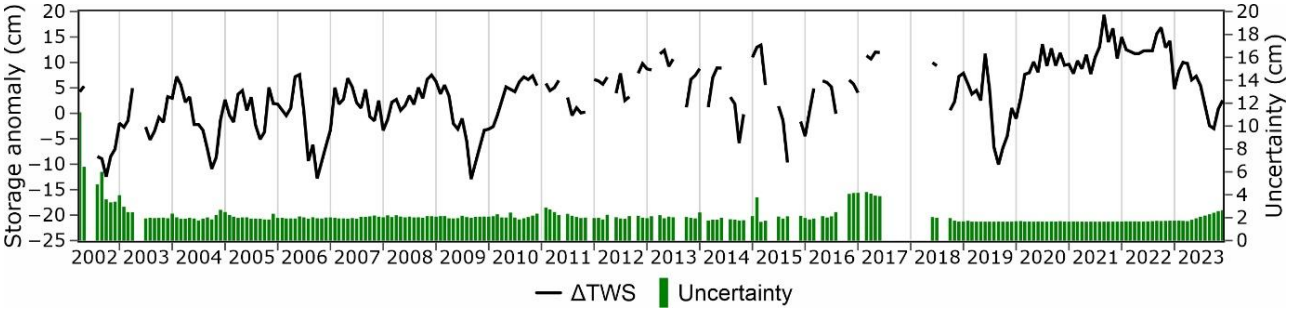

Figure S16: Uncertainty estimates for the 3° GRACE JPL grid in the study area.

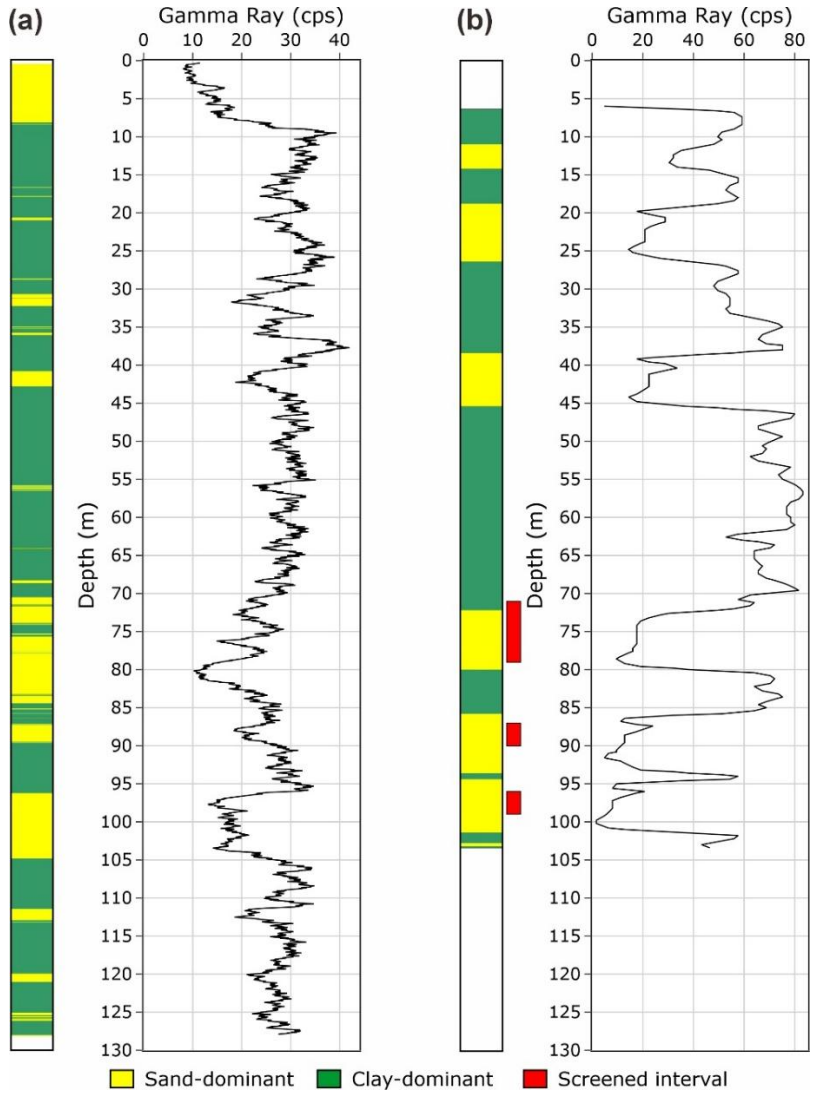

Figure S17: Lithological logs at (a) MG and (b) EBD sites.

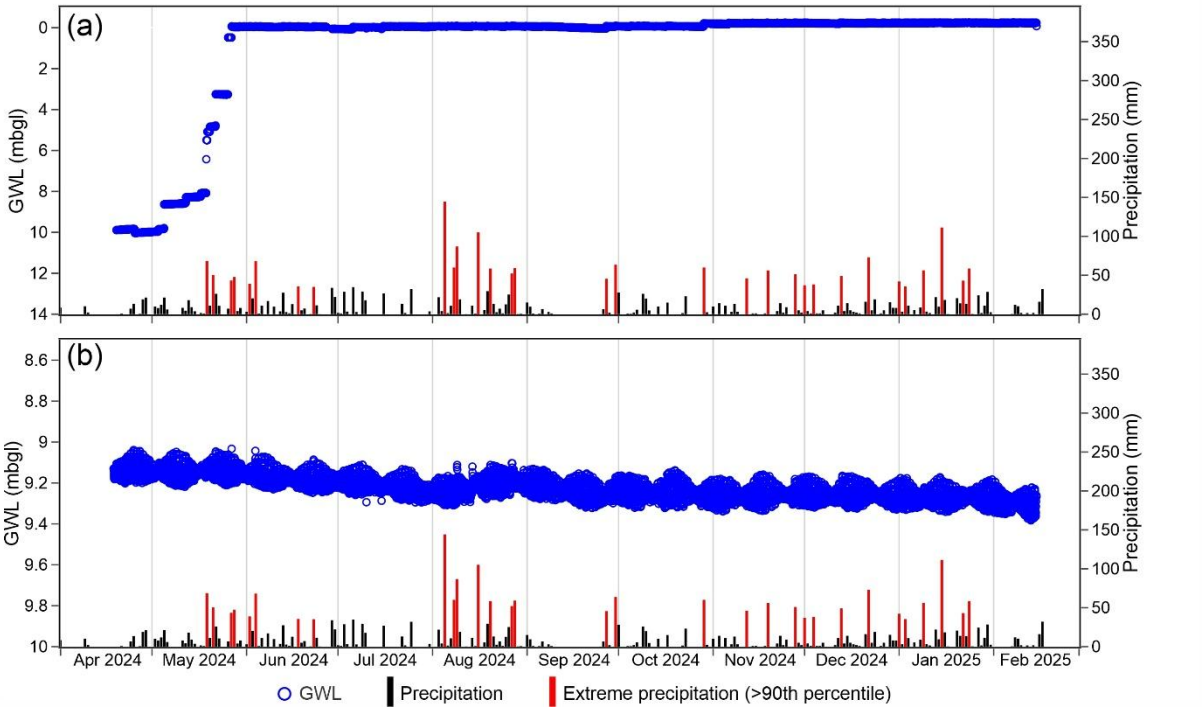

Figure S18: Comparison of hourly groundwater level (GWL) with daily precipitation from Balikpapan station at the MG site: (a) screened interval: 87-90 m, (b) screened interval: 132-135 m.

References

Indonesian Geological Survey: Pumping well database of Samarinda-Bontang Groundwater Basin [dataset], 2023.

Landerer, F. W. and Swenson, S. C.: Accuracy of scaled GRACE terrestrial water storage estimates, Water Resources Research, 48, https://doi.org/10.1029/2011WR011453, 2012.

Loomis, B. D., Luthcke, S. B., and Sabaka, T. J.: Regularization and error characterization of GRACE mascons, Journal of Geodesy, 93, 1381-1398, 10.1007/s00190-019-01252-y, 2019.

Pekel, J.-F., Cottam, A., Gorelick, N., and Belward, A. S.: High-resolution mapping of global surface water and its long-term changes, Nature, 540, 418-422, 10.1038/nature20584, 2016.

Save, H., Bettadpur, S., and Tapley, B. D.: High-resolution CSR GRACE RL05 mascons, Journal of Geophysical Research: Solid Earth, 121, 7547-7569, https://doi.org/10.1002/2016JB013007, 2016.

Watkins, M. M., Wiese, D. N., Yuan, D.-N., Boening, C., and Landerer, F. W.: Improved methods for observing Earth's time variable mass distribution with GRACE using spherical cap mascons, Journal of Geophysical Research: Solid Earth, 120, 2648-2671, https://doi.org/10.1002/2014JB011547, 2015.

Wiese, D. N., Landerer, F. W., and Watkins, M. M.: Quantifying and reducing leakage errors in the JPL RL05M GRACE mascon solution, Water Resources Research, 52, 7490-7502, https://doi.org/10.1002/2016WR019344, 2016.